Institutional Repository - Research Portal
Dépôt Institutionnel - Portail de la Recherche

researchportal.unamur.be

UNIVERSITÉ DE NAMUR

University of Namur

RESEARCH OUTPUTS / RÉSULTATS DE RECHERCHE

$^{18}O(p,\alpha)^{15}N$ isotopic tracing of germanium diffusion in SiO_2/Si films

Nelis, Adrien; Vickridge, Ian; Ganem, Jean-Jacques; Terwagne, Guy; Briand, Emrick

Published in:
Journal of Applied Physics

DOI:
10.1063/5.0057968

Publication date:
2021

Document Version
Publisher's PDF, also known as Version of record

Link to publication

Citation for pulished version (HARVARD):
Nelis, A, Vickridge, I, Ganem, J-J, Terwagne, G & Briand, E 2021, '$^{18}O(p,\alpha)^{15}N$ isotopic tracing of germanium diffusion in SiO_2/Si films', *Journal of Applied Physics*, vol. 130, no. 10, 105701. https://doi.org/10.1063/5.0057968

General rights
Copyright and moral rights for the publications made accessible in the public portal are retained by the authors and/or other copyright owners and it is a condition of accessing publications that users recognise and abide by the legal requirements associated with these rights.

- Users may download and print one copy of any publication from the public portal for the purpose of private study or research.
- You may not further distribute the material or use it for any profit-making activity or commercial gain
- You may freely distribute the URL identifying the publication in the public portal ?

Take down policy
If you believe that this document breaches copyright please contact us providing details, and we will remove access to the work immediately and investigate your claim.

Download date: 04. May. 2026

Journal of Applied Physics

$^{18}O(p,\alpha)^{15}N$ isotopic tracing of germanium diffusion in SiO_2/Si films

Cite as: J. Appl. Phys. **130**, 105701 (2021); https://doi.org/10.1063/5.0057968
Submitted: 26 May 2021 . Accepted: 14 August 2021 . Published Online: 08 September 2021

A. Nélis, I. Vickridge, J.-J. Ganem, E. Briand, G. Terwagne, et al.

View Online
Export Citation
CrossMark

© 2021 Author(s).

Journal of Applied Physics ARTICLE scitation.org/journal/jap

$^{18}O(p,\alpha)^{15}N$ isotopic tracing of germanium diffusion in SiO_2/Si films

Cite as: J. Appl. Phys. **130**, 105701 (2021); doi: 10.1063/5.0057968
Submitted: 26 May 2021 · Accepted: 14 August 2021 ·
Published Online: 8 September 2021

View Online Export Citation CrossMark

A. Nélis,[1,a)] I. Vickridge,[2] J.-J. Ganem,[2] E. Briand,[2] and G. Terwagne[1]

AFFILIATIONS

[1]LARN, Namur Institute of Structured Matter (NISM), University of Namur (UNAMUR), B-5000 Namur, Belgium
[2]Sorbonne Université, Institut des NanoSciences de Paris, CNRS UMR 7588, 4 place Jussieu, F-75252 Paris cedex 05, France

[a)]**Author to whom correspondence should be addressed:** adrien.nelis@unamur.be

ABSTRACT

We investigate the effects of oxygen on the thermal diffusion of germanium atoms, implanted inside a thermally grown SiO_2 layer, during high temperature processes (1100 °C, 60 min). The impact of the presence of oxygen on Ge diffusion is studied as a function of its origin, as it can come either from the annealing atmosphere (extrinsic source) or from the SiO_2 matrix itself (intrinsic source). ^{18}O labeling of the oxygen either in the annealing atmosphere or in the silica substrate, together with an isotopically sensitive ion beam analysis, shows a clear oxygen-dependence in germanium diffusion. This is especially so when oxygen is present in the annealing atmosphere, where it is responsible for an enhancement of germanium out-diffusion and redistribution into several peaks during annealing, through the formation of GeO molecules. A new three-process model is proposed to explain the impact of a contaminated atmosphere on the Ge redistribution. This is notably shown that a third Ge peak arises at the sample surface when the annealing atmosphere is contaminated by oxygen. This peak formation is explained by the oxidation of Ge present at the vicinity of the surface by oxygen coming from the annealing atmosphere. This is also shown that O_2 molecules can diffuse in depth, with a coefficient of diffusion $D_{O_2} \sim 10^{-9} cm^2/s$, until the densities of Ge and irradiation-induced defects increase, causing the progressive oxidation of Ge in depth and the restoration of the SiO_2 stoichiometry.

Published under an exclusive license by AIP Publishing. https://doi.org/10.1063/5.0057968

I. INTRODUCTION

Integration of germanium nanocrystals (Ge-ncs), and more widely group IV materials, produced by ion implantation into dielectric layers has been largely studied over the last few decades thanks to their numerous attractive optoelectronic properties.[1–5] Bandgap engineering, possible multiple exciton generation (MEG), and photoluminescence show great promise for enhancing the conversion efficiency of modern photovoltaic cells.

Fabrication of Ge-ncs by ion implantation requires thermal activation with temperatures as high as 800–1100 °C under a non-reactive atmosphere (N_2 or Ar), which is responsible for a long-range germanium redistribution inside the insulator layer, a thermally grown silicon dioxide film in this study.[6–14] Germanium diffusion mechanisms are generally associated in the literature to the presence of oxygen.[8–13,15,16] The first origin of the oxygen involved in germanium diffusion is the oxygen directly supplied by the SiO_2 host matrix and released by the dose-dependent damage and atomic rearrangement generated during the implantation and annealing processes. X-ray photoelectron spectroscopy (XPS) measurements demonstrated that implanted germanium ions are chemically bound to oxygen and silicon atoms present in the SiO_2 layer, already during the implantation process.[9,12,17] This is responsible for the formation of GeO_x compounds within the oxide film, including highly volatile GeO, considered to be the main contributor to germanium out-diffusion during thermal treatments. Heinig *et al.*[11] and Borodin *et al.*[18] also proposed that oxygen could be provided by the presence, in the annealing atmosphere, of residual moisture and other oxygen-containing compounds (O_2, H_2O, and OH). These oxidizing agents could penetrate through the damaged silica surface and diffuse inside the SiO_2 film.

In this work, we propose to use the ^{18}O isotope to trace oxygen behavior during thermal processes and to correlate it with the diffusion of implanted germanium atoms. Two sets of samples have been prepared. The first set of samples aims to highlight the transport of oxygen atoms originating in the SiO_2 layer by using an ^{18}O-containing oxide film implanted with Ge and annealed under a high purity N_2 atmosphere (100% of the gas introduced in the furnace tube). The second set of samples is intended to show the

Published under an exclusive license by AIP Publishing

impact of oxidizing agents present in the annealing environment on the diffusion of germanium by using commercial thermally grown SiO_2 layers implanted with germanium and annealed under a controlled atmosphere composed of 99% of nitrogen and 1% of $^{18}O_2$. This allows us to highlight the impact of the purity of the annealing environment on the germanium redistribution.

^{74}Ge and ^{18}O depth-distributions before and after annealing are obtained by a combination of Rutherford backscattering spectroscopy (RBS), nuclear reaction analysis (NRA), and resonant nuclear reaction analysis (RNRA) measurements.

II. EXPERIMENT

The two sets of samples will be referred as type A, for Ge implantations in $Si^{18}O_2$ layers (sandwiched between two $Si^{16}O_2$ layers—see below) annealed under pure N_2 (after the implantation), and type B, for Ge implantations in commercial SiO_2 films annealed under an atmosphere contaminated by $^{18}O_2$ molecules.

For type A samples, (100) silicon wafers are oxidized before Ge implantation under a dry atmosphere in three successive steps (^{16}O/^{18}O/^{16}O) to obtain a sandwich configuration. The respective thicknesses of the three layers (from the sample surface to depth), confirmed by RBS, were (1) ∼110 nm $Si^{16}O_2$; (2) ∼60 nm $Si^{18}O_2$; and (3) ∼80 nm $Si^{16}O_2$. They were chosen so that the projected range R_p of about 134 nm (calculated by SRIM-2013[19]) for the $^{74}Ge^+$ ions implanted at 185 keV is located around the middle of the ^{18}O labeled layer. After implantation, samples were annealed at 1100 °C for 60 min in pure N_2 (600 mbar) in a quartz tube furnace (INSP), coupled with a turbomolecular pump. The base pressure in the furnace before the introduction of N_2 was $<10^{-5}$ mbar.

For type B samples, 300 nm thick wet-oxidized and 200 nm dry-oxidized (100) silicon wafers were implanted with $^{74}Ge^+$ ions at energies of 230 keV ($R_p = 156$ nm) and 140 keV ($R_p = 156$ nm), respectively, for measured fluences varying from 3.5×10^{16} to 2.2×10^{17} Ge/cm^2. After implantation, the samples are annealed at 1100 °C for 60 min under a controlled atmosphere of 594 mbar N_2 plus 6 mbar $^{18}O_2$ in an INSP quartz tube furnace. Note that anneals just in 6 mbar $^{18}O_2$ without nitrogen give very similar results with a weak quantity of additional oxygen incorporated in the presence of nitrogen.

All implantations were carried out with the 2 MV Tandetron ALTAÏS (Accélérateur Linéaire Tandetron pour l'Analyse et l'Implantation des Solides) accelerator available at LARN.

^{74}Ge fluences and depth-profiles were verified by RBS before and after annealing at INSP with the 2.5 MV Van de Graaff accelerator of the SAFIR platform (System d'Analyses par Faisceaux d'Ions Rapides) or at LARN with ALTAÏS.

^{18}O depth-profiles were measured via the ^{18}O(p,α)^{15}N narrow resonant reaction (width $\Gamma \sim 100$ eV) at 151 keV.[20–23] The ^{18}O depth-profiles are deduced from the measured excitation curves by iteratively fitting simulations generated by SPACES,[24] assuming a stopping power and a density of 475 keV/(μg/cm^2) and 6.65×10^{22} at/cm^3, respectively, for pure SiO_2.

^{16}O and ^{18}O were quantified by NRA before and after annealing with ^{16}O(d,α)^{14}N and ^{18}O(d,α)^{16}N reactions at 860 and 750 keV.

III. RESULTS AND DISCUSSION

A. Annealing under pure N_2: Role of the host matrix

The isotopic sandwich structure of the implanted oxide is visible in Fig. 1, showing the ^{18}O depth-profile of a virgin ($Si^{16}O_2$/$Si^{18}O_2$/$Si^{16}O_2$) oxide layer represented by a black solid line. The $Si^{18}O_2$ film is centered at around 130 nm, almost corresponding to the middle of the whole oxide, with a small peak at the sample surface, resulting from ^{18}O/^{16}O exchanges taking place during successive oxidation steps.[25]

As shown in Fig. 1 for three different germanium fluences, the oxide layer undergoes a significant atomic rearrangement during implantation due to recoiled Si and O atoms and subsequent cascades of collisions caused by the passage of heavy $^{74}Ge^+$ ions. The beam effect is visible by observing the ^{18}O depth-distribution of the buried $Si^{18}O_2$ layer, showing substantial disorganization of the oxide film for the higher fluence (2.6×10^{17} Ge/cm^2—dotted line). This layer rearrangement is consistent with the changes in the SiO_2 stoichiometry calculated by Tridyn simulations in Ref. 9. This dose-dependent atomic rearrangement leads to large stoichiometric discrepancies throughout the SiO_2 film, resulting in silicon excess (with respect to stoichiometric SiO_2) between the sample surface and the Ge projected range and oxygen excess behind the projected range of germanium (see RBS results in Fig. S1 of the supplementary material and more details in Ref. 17). As a significant number of Si–O bonds are broken by the passage of the $^{74}Ge^+$ ions, a high fraction of $^{74}Ge^+$ ions will chemically bind to Si or O during the implantation. The concentrations of Ge–Si and Ge–O bonds increase with germanium fluences as well as the formation of Ge–Ge bonds[17] (see Fig. S2 in the supplementary material). Ge chemically bound to germanium or silicon is poorly mobile. The presence of germanium in an oxidized

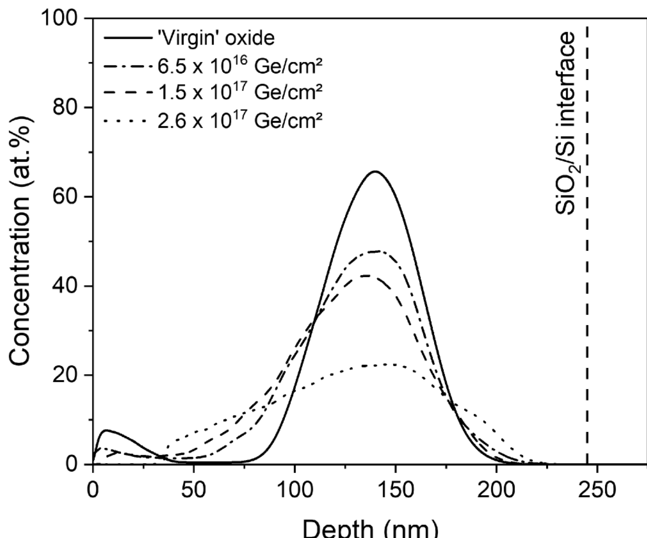

FIG. 1. ^{18}O depth-distributions of 245 nm $Si^{16}O/Si^{18}O/Si^{16}O$/Si layers for virgin oxide (solid line) and for implantation fluences of 6.5×10^{16}, 1.5×10^{17}, and 2.6×10^{17} Ge/cm^2. All profiles have as reference the SiO_2/Si interface.

Published under an exclusive license by AIP Publishing

state after the implantation step has been largely observed in literature studies.[9,12,17,26] Among GeO_x compounds, highly volatile GeO molecules are formed. These are generally considered to be the main mobile species responsible for both germanium diffusion and desorption.

As shown in Fig. 2, after implantation, both Ge and ^{18}O profiles practically overlap (black dots and blue solid lines, respectively). This allows us to study the migration of these two species and highlight a possible connection between their thermally activated diffusion. As germanium atoms locally bind with oxygen atoms to form GeO_x, a fraction of implanted ions chemically binds to ^{18}O and ^{16}O during the implantation.

Three implantation fluences of 6.5×10^{16}, 1.0×10^{17}, and 1.5×10^{17} Ge/cm^2 are shown in Fig. 2, corresponding to Figs. 2(a)–2(c), respectively. After annealing under a pure N_2 atmosphere, Ge exhibits a depth-profile (red triangles) consistent with that of samples annealed under pure N_2 (for example, see Ref. 7), i.e., a double peak configuration with a major peak slightly shifted toward the sample surface and an accumulation of Ge at the SiO_2/Si interface. This asymmetric diffusion is generally explained by the introduction of GeO molecules, diffusing toward oxygen-poor regions such as the sample surface and the SiO_2/Si interface.[8,9,11,17,27] The formation of these highly volatile GeO molecules could also explain Ge desorption occurring at the sample surface.

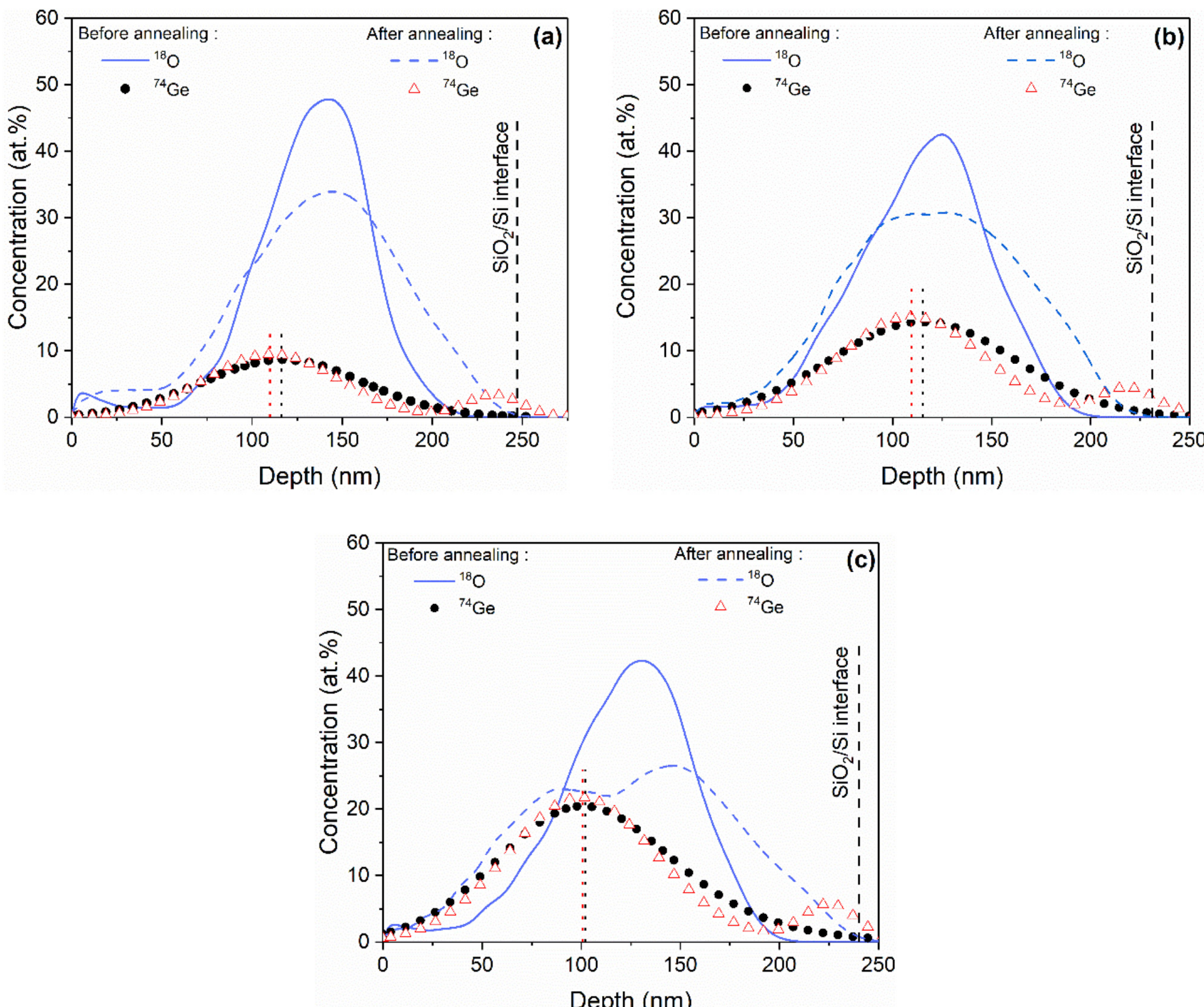

FIG. 2. ^{74}Ge depth-profiles, extracted from RBS spectra, before (black dots) and after (red triangles) annealing and ^{18}O RNRA depth-profiles before (blue solid line) and after (blue dashed line) annealing for (a) 6.5×10^{16}, (b) 1×10^{17}, and (c) 1.5×10^{17} Ge/cm^2. The depth position of the main peak is spotted by a dotted line.

Published under an exclusive license by AIP Publishing

We know from previous works that the mobility of Ge is linked to the saturation in oxygen of the SiO_2 layer. As the oxide region between the Ge projected range and the sample surface is under-stoichiometric (SiO_x, $x < 2$), metastable GeO_x will reduce in a thermodynamically more stable configuration, while the SiO_2 network tends to recover its stoichiometry [see Refs. 28 and 29 for Eq. (1), Ref. 16 for Eq. (2), and Ref. 30 for Eq. (3)],

$$GeO + SiO \rightarrow Ge + SiO_2, \tag{1}$$

$$GeO_x + Si \rightarrow Ge + SiO_x, \tag{2}$$

$$SiO_x \rightarrow \left(1-\frac{x}{2}\right)Si + \frac{x}{2}SiO_2. \tag{3}$$

All reactions are supposed to be initiated in the first moments of annealing. As the SiO_2 layer recovers its stoichiometry in a region initially presenting a lack of oxygen, the concentration of less mobile elemental Ge and Si increases, leading to the local formation of Ge and SiGe nanocrystals. As the coefficient of diffusion of Ge is two orders of magnitude higher than that of Si in SiO_2,[27] mostly, Ge–Si and Ge–Ge chemical bonds will be formed rather than Si–Si.[6,7,31] The chemical evolution of the main RBS peak has been probed by XPS studies,[16,17] confirming that GeO_x is reduced to elemental Ge^0 during annealing (i.e., Ge chemically bound to Ge or Si, which is not distinguishable by XPS). Only germanium implanted close to the surface is eventually able to desorb through the gas/oxide interface before being trapped by the nucleation process.

On the other side, a Ge accumulation peak is measured at the SiO_2/Si interface, indicating that a part of germanium diffuses inward. Due to the over-stoichiometric state (SiO_x, $x > 2$) of the oxide region between the Ge projected range and the Si substrate after implantation, the reduction process of Eqs. (1)–(3) will restore the SiO_2 stoichiometry while probably maintaining a mixture of elemental Ge and GeO_x compounds less likely to be trapped by Si dangling bonds because of oxygen excess. RBS analyses confirm that Ge mobility is greater in the second half of the Ge depth-profile, as it is this part of the profile that is redistributed during annealing.

The ^{18}O depth-profile after annealing (dashed blue lines) also shows an asymmetric diffusion whose range is limited to a few nanometers toward the sample surface but is, on the other hand, able to reach the SiO_2/Si interface. This is consistent with the stoichiometric discrepancies previously mentioned with a high rate of interactions of diffusing species with under-stoichiometric SiO_x ($x < 2$) between the Ge projected range and the sample surface, which acts as a trapping center for GeO_x ($0 \leq x < 2$) or oxygen, and with over-stoichiometric SiO_x ($x > 2$) toward the SiO_2/Si interface. Figure 2 shows that annealing perturbs the ^{18}O depth-profile more as the Ge fluence increases with a clear redistribution into two peaks for sample 2c. As observed by XPS (see Fig. S2 in the supplementay material), these positions correspond to the SiO_2 regions where the concentrations of elemental Ge and GeO_x are maximum after the implantation. These regions seem to be particular centers for oxygen fixation, due to trapping effects in under-stoichiometric regions and oxygen exchanges in over-stoichiometric regions.

As no real ^{18}O buildup is observed at the SiO_2/Si interface, it can be deduced that only a very small number of ^{18}O atoms reaches the substrate. Three possible interpretations are as follows:

1. The interface peak is due to the diffusion of elemental Ge whose diffusion in depth is not limited by the presence of silicon dangling bonds.
2. If germanium diffuses under the form of GeO_x compounds, this indicates that they could exchange or yield their oxygen before reaching the interface,

$$Ge^{18}O_x + Si^{16}O_2 \rightarrow Ge^{16}O_x + Si^{16(18)}O_2. \tag{4}$$

3. The number of Ge atoms chemically bound to ^{18}O is weak, as Ge will probably bind preferentially with recoiled ^{16}O coming from the first 110 nm.

Another possibility proposed in the literature is the encounter of GeO coming from the implanted zone and SiO molecules emitted by the substoichiometric interface,[9,15,32]

$$Ge^{18}O + Si^{16}O \rightarrow Ge + Si^{16(18)}O_2. \tag{5}$$

Knowing that the diffusion coefficient of SiO molecules is estimated to be $D_{SiO}(1100\,^{\circ}C) = 4 \times 10^{-17}\,cm^2/s$,[15] this can only occur close to the SiO_2/Si interface.

In any case, oxidized Ge would be reduced upon reaching the substoichiometric SiO_x/Si interface, releasing elemental Ge atoms in the vicinity of the SiO_2/Si interface, which is free to bond to Si (mainly) or other Ge atoms. At least, a part of this germanium is supposed to penetrate in a shallow layer of the silicon substrate because of the solubility of germanium in silicon due to their similar atomic structure.[8,11] This agrees with XPS observations,[12,17] indicating the presence of only Ge–Ge and Ge–Si chemical bonds in the vicinity of the interface region.

B. Annealing under a contaminated environment

Figure 3 shows Ge depth-profiles extracted from RBS analyses, before and after annealing, for type B samples implanted with different Ge fluences inside 200 nm [Fig. 3(a)] and 300 nm [Figs. 3(b)–3(d)] SiO_2 layers. Figures 3(b)–3(d) correspond to fluences of 4.5×10^{16}, 1.2×10^{17}, and 2.2×10^{17} Ge/cm^2, respectively. The fluence (3.5×10^{16} Ge/cm^2) of the sample presented in Fig. 3(a) has been chosen to get a similar concentration at maximum to that in the sample presented in Fig. 3(b). The left side of Figs. 3(a)–3(d) corresponds to the sample surface.

For each germanium fluence, the Ge depth-profile after annealing (red triangles in Fig. 3) is redistributed into three peaks with the emergence of a subsurface peak (peak 1) that was not observed for annealing under pure nitrogen (Fig. 2). This three-peak configuration, which is frequently observed in the literature,[8,10–12,17] is generally associated with the presence of oxygen in the annealing atmosphere.

As peak 1 is not present for annealing under pure N_2, this peak can be directly associated with the presence of oxygen in the annealing environment. Peaks 2 and 3 are similar to those observed in Fig. 2, corresponding to Ge diffusion mainly directed toward the sample surface and Ge accumulation at the SiO_2/Si interface but

Published under an exclusive license by AIP Publishing

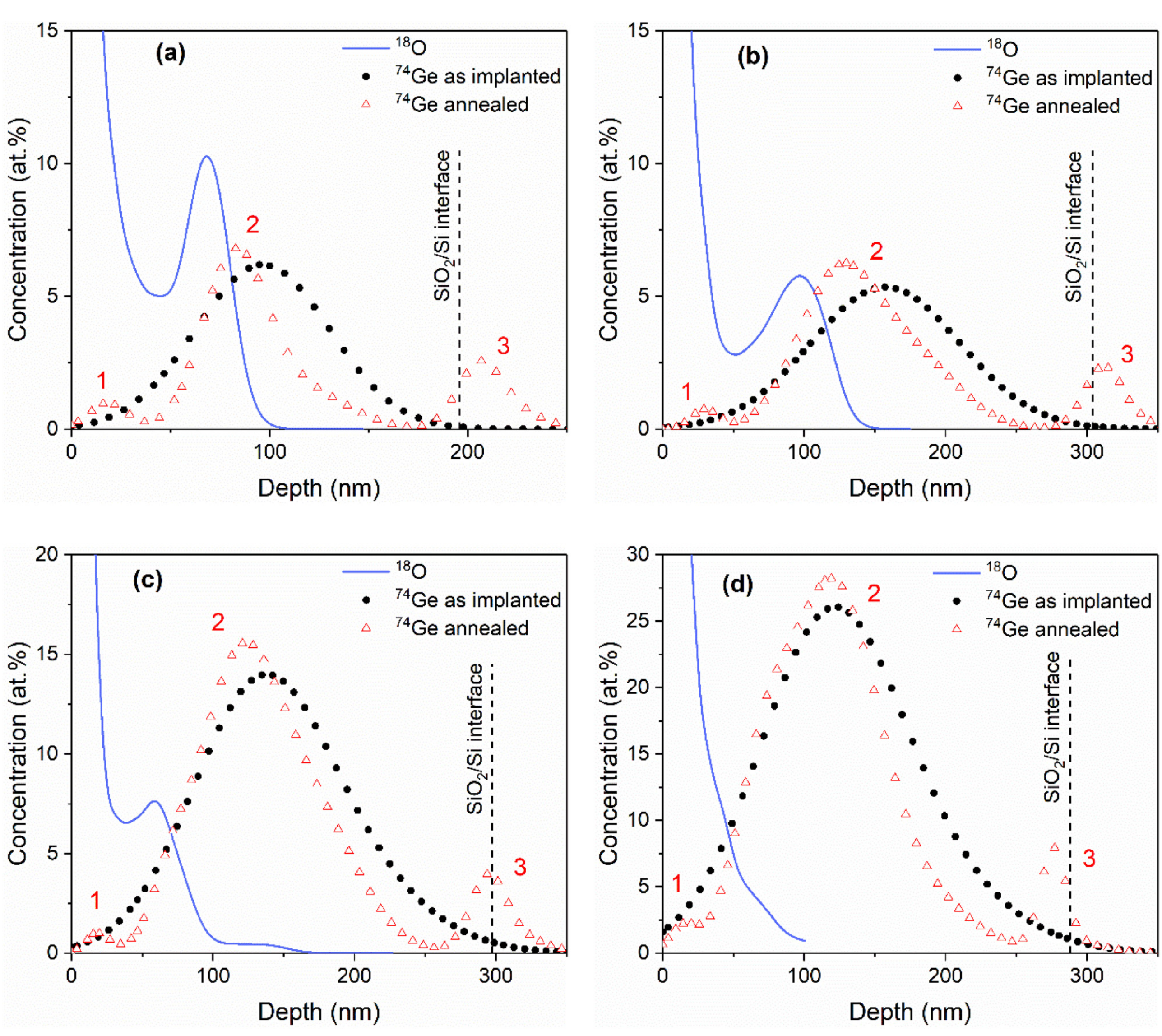

FIG. 3. ^{74}Ge depth-profiles, extracted from RBS spectra, before (black dots) and after (red triangles) annealing, ^{18}O RNRA deconvoluted depth-profiles after annealing (blue solid line) for fluencies of (a) 3.5×10^{16}, (b) 4.5×10^{16}, (c) 1.2×10^{17}, and (d) 2.2×10^{17} Ge/cm^2.

with a clear enhancement of outward diffusion for the intentionally contaminated atmosphere.

First of all, it can be inferred from NRA measurements (Fig. 4) that ^{18}O incorporation during annealing is not due only to ^{16}O/^{18}O surface exchanges since the total oxygen amount increases especially for the intermediate fluences. In this calculation, we suppose that each germanium atom desorbs in the form of GeO, carrying one oxygen atom while leaving the sample through the surface (orange boxes in Fig. 4). The amount of desorbing GeO molecules is deduced from Ge losses measured by RBS after annealing. NRA measurements will allow us to constrain the amount of ^{18}O in our RNRA fits.

In Ge-implanted SiO_2 layers, germanium mobility decreases as the fluence increases due to the formation of Ge–Si and Ge–Ge chemical bonds during implantation and annealing steps. Table I shows the decrease of Ge mobility, manifested by the reduction of the percentage of Ge in peaks 1 and 3, which obviously also depends on the relative distance with both interfaces.

^{18}O depth-profiles (blue solid lines) after annealing are superimposed on the Ge depth-profiles in Fig. 3 and fitted in Fig. 5 for

Published under an exclusive license by AIP Publishing

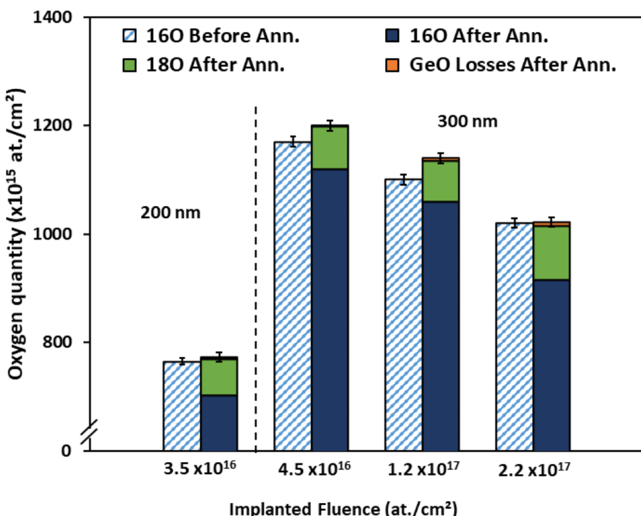

FIG. 4. Total oxygen atoms measured by $^{16}O(d,\alpha)^{14}N$ and $^{18}O(d,\alpha)^{16}N$ reactions for 200 (left) and 300 nm (right) SiO_2 before and after annealing. Orange boxes represent GeO desorption.

each fluence. ^{18}O depth-profiles, shown in Fig. 5, can be decomposed in three contributions (processes I, IIa, and IIb).

As the whole diffusion process is complex with the simultaneous diffusion of multiple species occurring at different rates, we will propose a possible explanation based on our experimental observations and literature.

A significant ^{18}O surface peak, noted process I, arises at the gas/SiO_2 interface and is attributed to the irradiation-induced damage and preferential sputtering of oxygen occurring at the sample surface during Ge implantation.[9,13,19,26] Process I depends on the implanted ion energy and fluence with a tail that extends from 25 to 50 nm. Therefore, a damaged oxygen-poor surface is exposed to $^{18}O_2$ during annealing, highly increasing the oxygen permeability of the surface.[9] Figure 5 shows that ^{18}O saturation is achieved at the extreme surface even for our low oxygen pressure. This surface will act as a constant oxygen provider.

Before annealing, the subsurface region is mainly composed of a mixture of partially oxidized silicon or germanium (SiO_x and GeO_x with $x < 2$) and elemental Ge (chemically bound to Ge or Si)

TABLE I. Percentage of Ge losses and contained in peaks 1 and 3 of Fig. 3 derived from RBS spectra and maximum displacement per atom as calculated by TRIM.

Fluence ($\times 10^{16}$ Ge/cm^2)	Ge losses (%)	Ge peak 1 (%)	Ge peak 3 (%)	Maximum displacement per atom (dpa)
3.5	12	6.4	19	55
4.5	2.5	3.7	14.4	72
12	4.2	1.4	9.6	199
22	2.7	1.5	7.9	366

whose concentration increases with the Ge fluence[17,26] (see two examples in Fig. S2 of the supplementary material). At 1100 °C, SiO_x is supposed to reduce within the first second of annealing[29] by Eq. (3). This agrees with the model of Borodin *et al.*,[18] considering only O_2 and the fraction of Ge that did not nucleate as the diffusing species. At the same time, $^{18}O_2$ penetrates the sample through the damaged surface and fully oxidizes all species present, or incoming, in the subsurface region, e.g., by reactions such as

$$2\,GeO + {}^{18}O_{2(g)} \rightarrow 2\,GeO_2, \tag{6}$$

$$Ge + {}^{18}O_{2(g)} \rightarrow GeO_2, \tag{7}$$

$$Si + {}^{18}O_{2(g)} \rightarrow SiO_2. \tag{8}$$

At the temperature considered in this work (1100 °C), Ge and Si oxidation occurs at the same time. However, SiO_2 is thermodynamically more stable than GeO_2 in systems involving Si, Ge, and O for which GeO_2 tends to reduce by reactions such as Eq. (2) in the presence of silicon even for weak Si concentrations.[33] Therefore, ^{18}O atoms will more favorably restore the SiO_2 stoichiometry [Eq. (8)] than form GeO_2. This passivation of silicon dangling bonds also enhances the diffusion of germanium by limiting the formation of Ge–Si bonds, favoring its desorption. RBS spectra show that germanium outward diffusion is initiated before its oxidation to immobile GeO_2, leading to the formation of peak 1. XPS studies confirmed that peak 1 is composed of fully oxidized germanium.[9,11,12,26] Zatsepin *et al.*[26] showed that each germanium atom, implanted near the sample surface (in the first 30–35 nm), is at least partially oxidized after 15 s of annealing at 950 °C, with a fraction of GeO_2/GeO_x ($x < 2$), which increases with the annealing time (approximately 40%–45% of Ge is fully oxidized after 1 min in these conditions). As the coefficients of diffusion increase with the temperature, the oxidation of germanium in the subsurface region will occur in a shorter time at 1100 °C.

Process I is fitted by an erfc function, resulting from the encounter of incompletely oxidized species and $^{18}O_2$ molecules,[22]

$$[^{18}O]_I(x,t) = \alpha\,\mathrm{erfc}(\beta x), \tag{9}$$

where α is the maximum concentration at the sample surface, almost constant for all samples, and β represents the dose-dependent peak width. $\beta = \frac{1}{2\sqrt{Dt}}$, with D being proportional to the concentration of incompletely oxidized species and their respective coefficient of diffusion.

As shown in Fig. 3, peak 1 overlaps with the tail of the ^{18}O surface peak, confirming an encounter between the oxygen molecules present in the annealing atmosphere, penetrating SiO_2 through the surface and diffusing inward and out-diffusing GeO_x compounds close to the surface. This is consistent with other works,[10–12] which suggested an overlapping between penetrating oxidizing agents and outgassing GeO, leading to the formation of fixed GeO_2 close to the sample surface.

Process IIa is hypothesized to be the result of the diffusion of $^{18}O_2$ molecules interacting with the Ge-implanted $Si^{16}O_2$

Published under an exclusive license by AIP Publishing

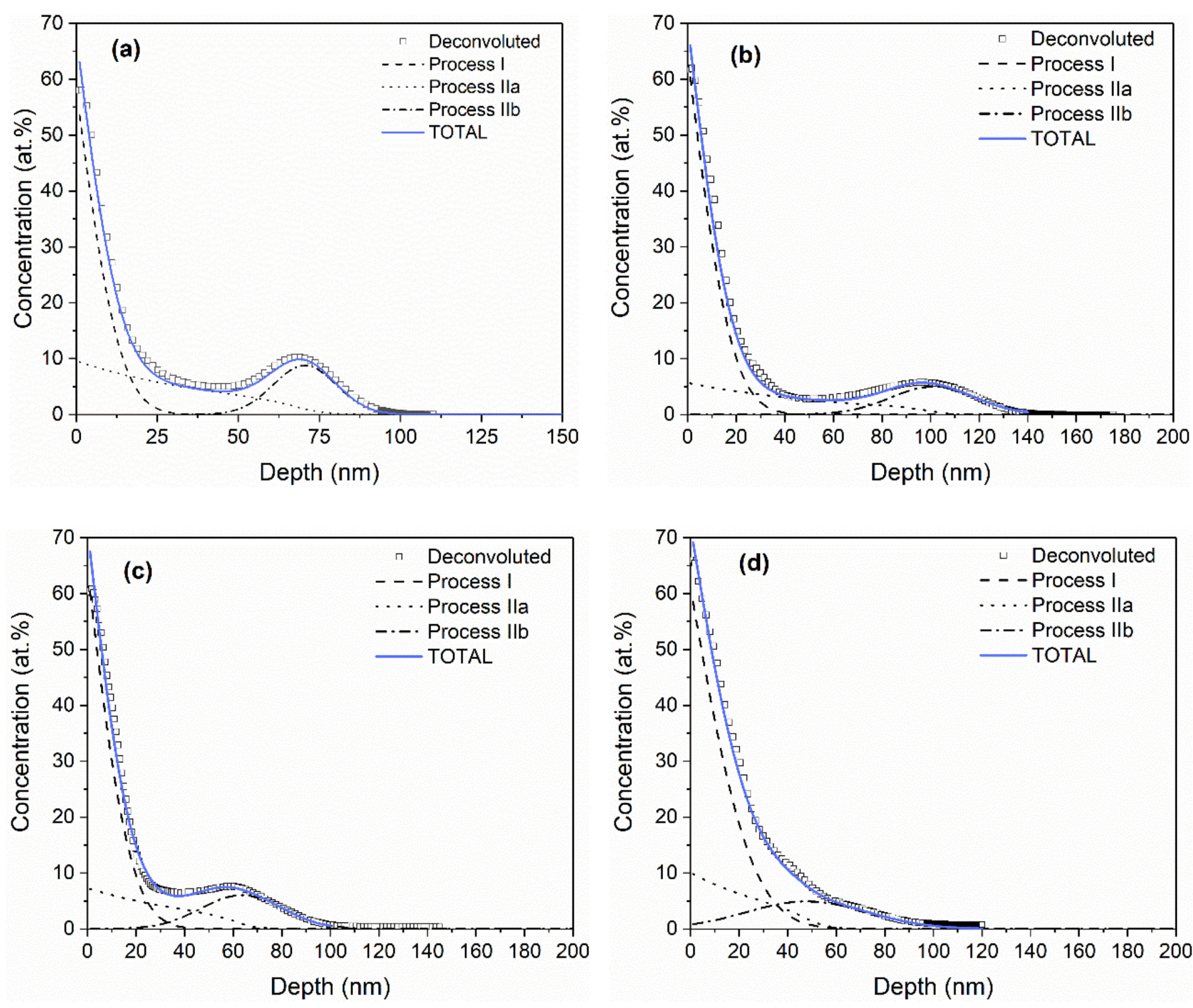

FIG. 5. Measured and deconvoluted (open squares) and calculated with processes I, IIa, and IIb (lines) ^{18}O RNRA depth-profiles for fluences of (a) 3.5 × 10^{16}, (b) 4.5 × 10^{16}, (c) 1.2 × 10^{17}, and (d) 2.2 × 10^{17} Ge/cm^2.

network. Process IIa is fitted using the following equation, presented in Ref. 21,

$$[^{18}O]_{IIa}(x, t) = L_g^{18}[^{18}O]_{c,x=0}\frac{\cos h[(x\text{-}x_0)/\lambda]}{\cos h(x_0/\lambda)}\,\gamma t, \qquad (10)$$

where L_g^{18} is the isotopic labeling of the employed gas, $[^{18}O]_{c,x=0}$ is the oxygen concentration at the sample surface (depending on the ^{18}O-enrichment and pressure of the gas and the solubility of ^{18}O in SiO_2[34]), x_0 is the oxide thickness, λ is the characteristic $^{16}O/^{18}O$ exchange length, and γ is the average rate at which a diffusing oxygen atom is exchanged with an oxygen atom of the $Si^{16}O_2$ network.

Using λ and γ parameters, we are able to calculate the $^{18}O_2$ diffusion coefficient by the following equation: $D_{O_2} = \gamma\lambda^2$. λ, γ, and D_{O_2} values are summarized in Table II for each sample. $D_{O_2}(1100\,^\circ C) \sim 10^{-9}\,cm^2/s$ is about one order of magnitude lower than the coefficient found by Norton in the case of a pure SiO_2 layer:[34] $1.2 \times 10^{-8}\,cm^2/s$ at 1078 °C. The difference could be explained by the morphological difference of our Ge-implanted samples compared to a pure SiO_2 layer, probably increasing the interactions between O_2 and the network. This is supported by the decrease of λ and D_{O_2} with the increase of the Ge fluence (Table II).

Process IIb, which is related to process IIa, is a buildup of inward diffusing ^{18}O whose integral and depth position appear to

Published under an exclusive license by AIP Publishing

TABLE II. Summary of integrals for processes I, IIa, and IIb with fitting parameters and calculated coefficient of diffusion.

		Process I	Process IIa				Process IIb	
Fluence ($\times 10^{16}$ Ge/cm^2)	Ox. thick. (nm)	$\sum_I$ (at./cm^2)	λ (nm)	γ (s^{-1})	D_{O_2} (cm^2/s)	$\sum_{IIa}$ (at./cm^2)	$\sum_{IIb}$ (at./cm^2)	x_C (nm)
3.5	200	3.06×10^{16}	50	59	1.48×10^{-9}	2.34×10^{16}	1.43×10^{16}	70.5
4.5	300	4.59×10^{16}	65	35	1.48×10^{-9}	1.91×10^{16}	1.46×10^{16}	101.0
12	300	4.50×10^{16}	50	49	1.31×10^{-9}	1.76×10^{16}	1.69×10^{16}	63.5
22	300	6.15×10^{16}	43	62	1.15×10^{-9}	1.90×10^{16}	2.00×10^{16}	48.0

be determined by the local concentration of Ge–Ge and Ge–Si chemical bonds, which dominates in peak 2, i.e., the oxide region where nanoclustering occurs.[10,11] Table II shows that, as the ^{74}Ge fluence increases, ^{18}O is trapped close to the surface in larger quantities. This is due to the local concentration of nonmobile Ge–Ge and Ge–Si chemical bonds (i.e., nanoclusters), which increases with the fluence until dominating the formation of GeO_x compounds during the implantation, as demonstrated by XPS in Ref. 17 (see Fig. S2 in the supplementary material; two examples are shown for Ge fluences of 0.80 and 1.30×10^{17} Ge/cm^2).

Process IIb is fitted by a Gaussian curve, whose integral is fixed by the total number of ^{18}O atoms present in the sample from the NRA measurements.

Under pure N_2, peak 2 (Fig. 3) corresponds to the region of nanoclustering, where mostly Ge–Ge or Ge–Si chemical bonds are observed.[6–8,10,12,13,17] When an oxygen contamination is present in the annealing environment, XPS and TEM measurements showed that peak 2 is gradually oxidized and the edge of the Ge nanocrystal band shifts to a greater depth with annealing time. For sufficient annealing time and oxygen supply, the complete oxidation of Ge nanocrystals can be achieved.[11,12,18]

This is consistent with our observations, showing that inward diffusing $^{18}O_2$ molecules react with Ge–Ge and Ge–Si bonds as soon as their concentrations increase. For longer annealing time, process IIb should continue to gradually overlap peak 2 until its complete oxidation. However, the shift of peak 2 toward the sample surface and the changes in its shape compared to pure N_2 annealing indicate that fixed GeO_2 is not directly formed. Two mechanisms must be considered. First, the presence of oxygen occupies Si dangling bonds, favoring Ge diffusion. Second, the formation of GeO_2 locally depends on the relative amounts of oxygen and germanium. Oxygen arrives gradually from the sample surface, while the local concentration of elemental germanium increases rapidly for the fluences used in this work. As GeO_2 is not stable in the presence of germanium at a high temperature ($GeO_2 + Ge \rightarrow 2GeO$),[33,35] a part of GeO molecules could diffuse toward the surface before being oxidized again in regions containing larger amounts of oxygen, either in peak 2 or near the sample surface (peak 1).

Considering the coefficient of diffusion deduced from process IIa, $D_{O_2}(1100\,^\circ C)$, the number of ^{18}O atoms at a certain depth Δx after an annealing time t, maintaining a constant concentration of ^{18}O at the sample surface, is given by

$$n_{^{18}O}(x, t) = L_g^{18}[^{18}O]_{c,x=0} D_{O_2}(1100\,^\circ C)\frac{t}{\Delta x}. \qquad (11)$$

This allows us to estimate the quantity of ^{18}O atoms, which should accumulate by process IIb. As the integral of process IIb is systematically lower than this calculated value $n_{^{18}O}(x, t)$ for each sample, this supports the idea of an out-diffusion of Ge^{18}O, enhanced by the presence of oxygen in the annealing atmosphere.

Considering the weak isotopic labeling of the SiO_2 layer after annealing, corresponding to less than 8% of the total oxygen amount, we assume that processes I and II are independent.

No measurable ^{18}O accumulation has been observed at the SiO_2/Si interface, indicating that all $^{18}O_2$ is consumed in the Ge oxidation process of peak 2. Therefore, peak 3, in the vicinity of the SiO_2/Si interface, is rather more influenced by the oxide thickness and the Ge fluence than the presence of ^{18}O in the annealing atmosphere. For a similar atomic concentration, Ge buildup at the interface is more significant for thinner samples (Table I), which can be explained by the proximity to the SiO_2/Si interface and the lower implantation fluence.

IV. CONCLUSIONS

We studied the origin of oxygen involved in germanium diffusion into a SiO_2/Si layer by a combination of stable isotopic tracing and three ion beam analysis (IBA) techniques: RBS, RNRA, and NRA.

A new experimental proof is provided that, compared to a pure N_2 environment, a low percentage of O_2 in the annealing atmosphere enhances Ge out-diffusion through the formation of GeO molecules. It is shown that this oxygen contamination causes the oxidation of diffusing species close to the sample surface, as well as in the region of nanocrystal growth, in agreement with models proposed in the literature. This underlines the importance of working in pure and non-reactive atmospheres.

SUPPLEMENTARY MATERIAL

See the supplementary material for RBS analyses highlighting the changes in the SiO_2 stoichiometry after the Ge implantation (Fig. S1). Figure S2 shows Ge depth-profiles in SiO_2 measured by XPS for two different Ge fluences. The chemical state of implanted Ge ions after the implantation is shown in Fig. S2.

ACKNOWLEDGMENTS

This work was made possible thanks to the Fédération Wallonie-Bruxelles (FWB) travel grant (No. BV17-54). The authors would like to thank the SIAM (Synthesis, Irradiation and Analysis of Materials) technological platform for the use of ALTAÏS and

Published under an exclusive license by AIP Publishing

T. Tabarrant for his technical support on the accelerator. This work had benefited from access to the SAFIR platform of the CNRS and the Sorbonne University. A.N. would like to personally thank Hervé Tancrez.

DATA AVAILABILITY

The data that support the findings of this study are available from the corresponding author upon reasonable request.

REFERENCES

[1] M. A. Green and S. P. Bremner, "Energy conversion approaches and materials for high-efficiency photovoltaics," Nat. Mater. **16**, 23–34 (2017).

[2] M. Yedji, J. Demarche, G. Terwagne, R. Delamare, D. Flandre, D. Barba, D. Koshel, and G. G. Ross, "Method for fabricating third generation photovoltaic cells based on Si quantum dots using ion implantation into SiO_2," J. Appl. Phys **109**(8), 084337 (2011).

[3] M. C. Beard, K. P. Knustsen, P. Yu, Q. Song, J. Luther, R. Ellingson, and A. J. Nozik, "Multiple exciton generation in colloidal silicon nanocrystals," Nano Lett. **7**, 2506–2512 (2007).

[4] M. T. Trinh, R. Limpens, W. D. A. M. de Boer, J. M. Schins, L. D. A. Siebbeles, and T. Gregorkiewicz, "Direct generation of multiple excitons in adjacent silicon nanocrystals revealed by induced absorption," Nat. Photonics **6**(5), 316–321 (2012).

[5] C. Smith and D. Binks, "Multiple exciton generation in colloidal nanocrystals," Nanomaterials **4**(1), 19–45 (2013).

[6] D. Barba, C. Wang, A. Nélis, G. Terwagne, and F. Rosei, "Blocking germanium diffusion inside silicon dioxide using a co-implanted silicon barrier," J. Appl. Phys. **123**(16), 161540 (2018).

[7] A. Nélis, D. Barba, and G. Terwagne, "Control of germanium diffusion using low quantities of co-implanted silicon isotopes," J. Appl. Phys. **128**(12), 125705 (2020).

[8] A. Markwitz, B. Schmidt, W. Matz, R. Grötzschel, and A. Mücklich, "Microstructural investigation of ion beam synthesised germanium nanoclusters embedded in SiO_2 layers," Nucl. Instrum. Methods Phys. Res. B **142**(3), 338–348 (1998).

[9] V. Beyer and J. von Borany, "Elemental redistribution and Ge loss during ion-beam synthesis of Ge nanocrystals in SiO_2 films," Phys. Rev. B **77**(1), 014107 (2008).

[10] J. von Borany, R. Grötzschel, K. H. Heinig, A. Markwitz, W. Matz, B. Schmidt, and W. Skorupa, "Multimodal impurity redistribution and nanocluster formation in Ge implanted silicon dioxide films," Appl. Phys. Lett. **71**(22), 3215–3217 (1997).

[11] K. H. Heinig, B. Schmidt, A. Markwitz, R. Grötzschel, M. Strobel, and S. Oswald, "Precipitation, ripening and chemical effects during annealing of Ge+ implanted SiO_2 layers," Nucl. Instrum. Methods Phys. Res. B **148**(1–4), 969–974 (1999).

[12] S. Oswald, B. Schmidt, and K.-H. Heinig, "XPS investigation with factor analysis for the study of Ge clustering in SiO_2," Surf. Interface Anal. **29**(4), 249–254 (2000).

[13] D. Barba, R. S. Cai, J. Demarche, Y. Q. Wang, G. Terwagne, F. Rosei, and G. G. Ross, "Influence of silicon dangling bonds on germanium thermal diffusion within SiO_2 glass," Appl. Phys. Lett. **104**(11), 111901 (2014).

[14] V. Baranwal, J. W. Gerlach, A. Lotnyk, B. Rauschenbach, H. Karl, S. Ojha, D. K. Avasthi, D. Kanjilal, and A. C. Pandey, "Embedded Ge nanocrystals in SiO_2 synthesized by ion implantation," J. Appl. Phys. **118**(13), 134303 (2015).

[15] M. Uematsu, H. Kageshima, Y. Takahashi, S. Fukatsu, K. M. Itoh, K. Shiraishi, and U. Gösele, "Modeling of Si self-diffusion in SiO_2: Effect of the Si/SiO_2 interface including time-dependent diffusivity," Appl. Phys. Lett. **84**(6), 876–878 (2004).

[16] W. K. Choi, V. Ho, V. Ng, Y. W. Ho, S. P. Ng, and W. K. Chim, "Germanium diffusion and nanocrystal formation in silicon oxide on silicon substrate under rapid thermal annealing," Appl. Phys. Lett. **86**(14), 143114 (2005).

[17] A. Nélis, E. Haye, and G. Terwagne, "Influence of oxygen co-implantation on germanium out-diffusion and nanoclustering in SiO_2/Si films," Thin Solid Films (in press) (2021).

[18] V. A. Borodin, K. H. Heinig, and B. Schmidt, "Modeling of Ge nanocluster evolution in ion-implanted SiO_2 layer," Nucl. Instrum. Methods Phys. Res. B **147**(1–4), 286–291 (1999).

[19] J. F. Ziegler, M. D. Ziegler, and J. P. Biersack, "SRIM—The stopping and range of ions in matter (2010)," Nucl. Instrum. Methods Phys. Res. B **268**(11–12), 1818–1823 (2010).

[20] G. Amsel and D. Samuel, "Microanalysis of the stable isotopes of oxygen by means of nuclear reactions," Anal. Chem. **39**(14), 1689–1698 (1967).

[21] C. D. Cavellin, I. Trimaille, J. J. Ganem, M. D'Angelo, I. Vickridge, A. Pongracz, and G. Battistig, "An ^{18}O study of the interaction between carbon monoxide and dry thermal SiO_2 at 1100 °C," J. Appl. Phys. **105**(3), 033501 (2009).

[22] I. Trimaille and S. Rigo, "Use of ^{18}O isotopic labelling to study thermal dry oxidation of silicon as a function of temperature and pressure," Appl. Surf. Sci. **39**(1–4), 65–80 (1989).

[23] G. Battistig, G. Amsel, E. d'Artemare, and I. Vickridge, "A very narrow resonance in 18O(p, α)15 N near 150 keV application to isotopic tracing. I. Resonance width measurement," Nucl. Instrum. Methods Phys. Res. B **61**(4), 369–376 (1991).

[24] I. Vickridge and G. Amsel, "SPACES: A PC implementation of the stochastic theory of energy loss for narrow-resonance depth profiling," Nucl. Instrum. Methods Phys. Res. B **45**(1–4), 6–11 (1990).

[25] J.-J. Ganem, I. Trimaille, P. André, S. Rigo, F. C. Stedile, and I. J. R. Baumvol, "Diffusion of near surface defects during the thermal oxidation of silicon," J. Appl. Phys. **81**(12), 8109–8111 (1997).

[26] A. F. Zatsepin, D. A. Zatsepin, I. S. Zhidkov, E. Z. Kurmaev, H. J. Fitting, B. Schmidt, A. P. Mikhailovich, and K. Lawniczak-Jablonska, "Formation of Ge 0 and GeO x nanoclusters in Ge+-implanted SiO_2/Si thin-film heterostructures under rapid thermal annealing," Appl. Surf. Sci. **349**, 780–784 (2015).

[27] M. V. Minke and K. A. Jackson, "Diffusion of germanium in silica glass," J. Non-Cryst. Solids **351**(27–29), 2310–2316 (2005).

[28] M. P. Gambaryan, G. K. Krivyakin, S. G. Cherkova, M. Stoffel, H. Rinnert, M. Vergnat, and V. A. Volodin, "Quantum size effects in germanium nanocrystals and amorphous nanoclusters in $GeSi_xO_y$ films," Phys. Solid State **62**(3), 492–498 (2020).

[29] V. A. Dan'ko, "Kinetics of structural and phase transformations in thin SiOx films in the course of a rapid thermal annealing," Semiconductors **39**(10), 1197 (2005).

[30] K. Prabhakaran, F. Maeda, Y. Watanabe, and T. Ogino, "Distinctly different thermal decomposition pathways of ultrathin oxide layer on Ge and Si surfaces," Appl. Phys. Lett. **76**(16), 2244–2246 (2000).

[31] D. Barba, J. Demarche, F. Martin, G. Terwagne, and G. G. Ross, "Trapping of diffusing germanium by silicon excess co-implanted into fused silica," Appl. Phys. Lett. **101**(14), 143107 (2012).

[32] Y. Takakuwa, M. Nihei, and N. Miyamoto, "Out diffusion and subsequent desorption of volatile SiO molecules during annealing of thick SiO_2 films in vacuum," Jpn J. Appl. Phys. **32**(Part 2, No. 4A), L480–L483 (1993).

[33] P.-E. Hellberg, S.-L. Zhang, F. M. D'Heurle, and C. S. Petersson, "Oxidation of silicon–germanium alloys. II. A mathematical model," J. Appl. Phys. **82**(11), 5779–5787 (1997).

[34] F. J. Norton, "Permeation of gaseous oxygen through vitreous silica," Nature **191**(4789), 701–701 (1961).

[35] J. Oh and J. C. Campbell, "Thermal desorption of Ge native oxides and loss of Ge from the surface," J. Electon. Mater. **33**(4), 364–367 (2004).

Published under an exclusive license by AIP Publishing